Constraints on the Invariant Functions of Axisymmetric Turbulence

E. J. Kerschen*
General Electric Company, Schenectady, New York

Constraints are derived for the two invariant functions Q_1 and Q_2 that occur in Chandrasekhar's development of the axisymmetric turbulence theory. These constraints must be satisfied for the correlation tensor derived from Q_1 and Q_2 to be that of a stationary random process, i.e., for the turbulence to be realizable. The equivalent results in spectrum space are also developed. Applications of the constraints in aerodynamic noise modeling are discussed. It is shown that significant errors in prediction can be introduced by the use of turbulence models which violate the constraints.

I. Introduction

THE statistical theory of homogeneous turbulence had its beginnings in the work of Taylor,[1,2] who introduced the assumption of isotropy. For isotropic turbulence the velocity correlation tensor, $R_{ij}=\langle u_i u_j' \rangle$, is invariant under arbitrary rotations and reflections of the coordinate axes. Here u_i and u_j' are the x_i and x_j components of the velocities at points $\boldsymbol{P}$ and $\boldsymbol{P}'$, respectively, and the brackets $\langle\ \rangle$ denote an ensemble average. Taylor's analysis was extended by von Kármán[3,4] and von Kármán and Howarth[5] who showed that for isotropic turbulence the velocity correlation tensor can be expressed in terms of a single scalar function Q. The function Q depends only on the magnitude r of $\boldsymbol{x}=\boldsymbol{P}'-\boldsymbol{P}$. The theory of isotropic turbulence has been developed extensively in the intervening years, contributing significantly to the understanding of basic turbulence phenomena. The results of the isotropic turbulence theory have also been applied to the calculation of problems such as turbulent diffusion and aerodynamic sound generation.

The simplest generalization of isotropic turbulence is axisymmetric turbulence, in which we assume that the flowfield has a preferred direction. Thus the correlation tensor is invariant only for rotations about the preferred direction (λ) and for reflections in planes containing λ and perpendicular to λ. Axisymmetric and isotropic turbulence are both artificial situations that are at best only approximate models of actual turbulent flows. Most turbulent flows have more than one preferred direction and do not satisfy the condition of homogeneity. However, in many cases, homogeneous turbulence provides a reasonable first approximation to the flow. In support of this staement, it might be relevant to note that second-order (invariant) turbulence modeling appears to be an orderly expansion about homogeneous turbulence.[6] While axisymmetric and isotropic turbulence are both homogeneous, axisymmetric turbulence has the important advantage that anisotropy is included in the model. Thus the axisymmetric turbulence theory can be used to model the fluid motion in situations where the isotropic theory is inadequate.

Axisymmetric turbulence theory has been utilized in fundamental turbulence research and for modeling turbulent flows and their by-products. Herring[7] and Schumann and Patterson[8] examined the return to isotropy of axisymmetric turbulence. The effect of a rapid distortion on axisymmetric turbulence was investigated by Sreenivasan and Narasimha.[9] The latter also present comparisons of experimental data and axisymmetric turbulence models for a variety of flows. They find that axisymmetric theory provides reasonably accurate models for the turbulence at the centerlines of pipes and channels, in the outer part of a constant-pressure boundary layer, and in nearly homogeneous shear flow. Hassan et al.[10] extended the axisymmetric model of pipe flow turbulence to include off-center locations and obtained very good agreement with isocorrelation contour measurements. In their study of jet noise, Goldstein and Rosenbaum[11] used data from several experiments to support axisymmetric turbulence as a model for limited regions of jets. The inlet flow occurring in ground-based fan test facilities generally corresponds closely to an axisymmetric contraction of isotropic turbulence. Fan noise analyses incorporating turbulence distortion due to the inlet contraction have been presented by Goldstein et al.,[12] Mani and Bekofske,[13] and Kerschen and Gliebe.[14]

The earliest development of axisymmetric turbulence theory was presented by Batchelor.[15] He used invariant theory to show that the velocity correlation tensor could be expressed in terms of four scalar functions depending on both r and $\boldsymbol{x}\cdot\boldsymbol{\lambda}$. Application of the continuity equation then produced two partial differential equations relating these four functions. However, the complexity of the differential equations precluded their use in eliminating two of the scalar functions. Chandrasekhar[16] further extended the analysis of axisymmetric turbulence and obtained an explicit representation of R_{ij} in terms of two scalar functions, Q_1 and Q_2, of r and $\boldsymbol{x}\cdot\boldsymbol{\lambda}$. He achieved this representation by expressing the velocity correlation tensor as the curl of a skew tensor. This approach automatically satisfies the continuity equation.

In deriving the general form of the velocity correlation tensor, Batchelor and Chandrasekhar essentially used only kinematic and symmetry requirements. Their analyses showed that Q_1 and Q_2 were even functions of the variables r and $\boldsymbol{x}\cdot\boldsymbol{\lambda}$, and that the lower order terms of the expansions about the origin were related to certain physically measurable quantities. With the exception of these requirements, the functional behavior of Q_1 and Q_2 on r and $\boldsymbol{x}\cdot\boldsymbol{\lambda}$ was considered to be arbitrary. However, a fundamental statistical theorem established by Cramer[17] places certain constraints on the velocity correlation tensor. Specifically, he shows that the energy spectrum tensor (obtained by taking the Fourier transform of R_{ij}) must have a non-negative quadratic form. In the present paper, the results of Cramer are used to obtain constraints which the invariant functions Q_1 and Q_2 must satisfy. The equivalent results in spectrum space are also presented. These constraints are particularly useful for applications of the axisymmetric turbulence theory to the modeling of processes such as dispersion or aerodynamic sound generation, where the functions Q_1 and Q_2 must be

Received April 26, 1982; revision received Nov. 16, 1982.

*Mechanical Engineer, Corporate Research and Development. (Presently Assistant Professor, University of Arizona, Tucson, Arizona.) Member AIAA.

given assumed forms. The constraints then provide a guide as to the reasonableness of the assumed forms. Applications in the field of aerodynamic noise are discussed, and it is shown that violation of the constraints can lead to significant errors in prediction.

II. Invariant Function Relationships

In this section, the relationships between the functions Q_1 and Q_2 in Chandrasekhar's development of axisymmetric turbulence and the corresponding invariant functions in spectrum space are derived. Chandrasekhar showed that the velocity correlation tensor R_{ij} could be derived from

$$R_{ij}(x) = \epsilon_{jlm}\frac{\partial q_{im}}{\partial x_l} \tag{1a}$$

where

$$q_{ij} = Q_1\epsilon_{ijk}x_k + Q_2\lambda_j\epsilon_{ilm}\lambda_l x_m + \frac{1}{r}\frac{\partial Q_1}{\partial \mu}x_j\epsilon_{ilm}\lambda_l x_m \tag{1b}$$

Here ϵ_{ijk} is the alternating tensor, $\lambda\cdot x = r\mu$, and Q_1 and Q_2 are functions of r and $r\mu$. Note that the above representation automatically satisfies the continuity equation. If we assume that λ lies in the positive x_1 direction and introduce the variable $\sigma = (x_2^2 + x_3^2)^{1/2}$ such that Q_1 and Q_2 are functions of x_1 and σ, we obtain the following results:

$$R_{11} = -2Q_1 - \sigma\frac{\partial Q_1}{\partial \sigma} \tag{2a}$$

$$R_{12} = R_{21} = x_2\frac{\partial Q_1}{\partial x_1}, \qquad R_{13} = R_{31} = x_3\frac{\partial Q_1}{\partial x_1} \tag{2b}$$

$$R_{22} = -2Q_1 - Q_2 - 2x_1\frac{\partial Q_1}{\partial x_1} - 2x_3\frac{\partial Q_1}{\partial x_3} - x_3\frac{\partial Q_2}{\partial x_3} + x_3^2\frac{\partial^2 Q_1}{\partial x_1^2} - 2x_1x_3\frac{\partial^2 Q_1}{\partial x_1\partial x_3} + x_1^2\frac{\partial^2 Q_1}{\partial x_3^2} \tag{2c}$$

$$R_{33} = -2Q_1 - Q_2 - 2x_1\frac{\partial Q_1}{\partial x_1} - 2x_2\frac{\partial Q_1}{\partial x_2} - x_2\frac{\partial Q_2}{\partial x_2} + x_2^2\frac{\partial^2 Q_1}{\partial x_1^2} - 2x_1x_2\frac{\partial^2 Q_1}{\partial x_1\partial x_2} + x_1^2\frac{\partial^2 Q_1}{\partial x_2^2} \tag{2d}$$

$$R_{23} = R_{32} = x_2x_3\left[\frac{2}{\sigma}\frac{\partial Q_1}{\partial \sigma} + \frac{1}{\sigma}\frac{\partial Q_2}{\partial \sigma} + \frac{2x_1}{\sigma}\frac{\partial^2 Q_1}{\partial \sigma\partial x_1} - \frac{x_1^2}{\sigma}\frac{\partial}{\partial \sigma}\left(\frac{1}{\sigma}\frac{\partial Q_1}{\partial \sigma}\right) - \frac{\partial^2 Q_1}{\partial x_1^2}\right] \tag{2e}$$

We will now derive the corresponding results in spectrum space. Batchelor used invariant theory and symmetry requirements to show that the velocity correlation tensor must have the form

$$R_{ij} = C_1x_ix_j + C_2\delta_{ij} + C_3\lambda_i\lambda_j + C_4(\lambda_ix_j + x_i\lambda_j) \tag{3}$$

where the C_i, $i=1,\ldots,4$, are functions of r and $x\cdot\lambda$. Introducing the energy spectrum tensor

$$\Phi_{ij}(k) = \frac{1}{(2\pi)^3}\int_{-\infty}^{\infty}\!\!\int\!\!\int R_{ij}(x)e^{-ik\cdot x}\,dx \tag{4}$$

we have the equivalent representation

$$\Phi_{ij} = D_1k_ik_j + D_2\delta_{ij} + D_3\lambda_i\lambda_j + D_4(\lambda_ik_j + k_i\lambda_j) \tag{5}$$

where the D_i, $i=1,\ldots,4$, are functions of $k=|k|$ and $k\cdot\lambda$. Equations (3) and (5) for R_{ij} and Φ_{ij} do not satisfy the continuity equation for arbitrary choices of C_i and D_i. Applying the continuity equation ($\partial R_{ij}/\partial x_j = 0$) to Eq. (3) produces two partial differential equations involving the four functions C_i. It was this difficulty which led Chandrasekar to represent R_{ij} as the curl of a skew tensor. Applying the continuity equation in spectrum space leads to no such difficulties, since derivatives are not involved. Thus, setting $k_j\Phi_{ij} = 0$, we obtain

$$k_i[D_1k^2 + D_2 + D_4k_m\lambda_m] + \lambda_i[D_3k_m\lambda_m + D_4k^2] = 0$$

This equation must be satisfied for arbitrary choices of k_i and λ_i, and thus the two expressions in square brackets vanish identically. Using these to eliminate D_2 and D_4 and setting $F = D_3/k^2 - D_1$, $G = -D_3/k^2$, we obtain,

$$\Phi_{ij} = \{k^2\delta_{ij} - k_ik_j\}F + \{[k^2 - (k_m\lambda_m)^2]\delta_{ij} - k_ik_j - k^2\lambda_i\lambda_i + k_m\lambda_m(\lambda_ik_j + k_i\lambda_j)\}G \tag{6}$$

Let λ lie in the positive k_1 direction, we obtain

$$\Phi_{11} = (k_2^2 + k_3^2)F \tag{7a}$$

$$\Phi_{12} = \Phi_{21} = -k_1k_2F, \qquad \Phi_{13} = \Phi_{31} = -k_1k_3F \tag{7b}$$

$$\Phi_{22} = (k_1^2 + k_3^2)F + k_3^2G \tag{7c}$$

$$\Phi_{33} = (k_1^2 + k_2^2)F + k_2^2G \tag{7d}$$

$$\Phi_{23} = \Phi_{32} = -k_2k_3(F+G) \tag{7e}$$

where F and G are considered to be functions of k_1 and $k_t = (k_2^2 + k_3^2)^{1/2}$.

We now wish to relate the functions $Q_1(x)$ and $Q_2(x)$ to $A(x)$ and $B(x)$, where A and B are the inverse Fourier transforms of F and G, i.e.,

$$A(x) = \int_{-\infty}^{\infty}\!\!\int\!\!\int F(k)e^{ik\cdot x}\,dk, \text{ etc.}$$

Consider first the relationship between Q_1 and A. Taking the inverse Fourier transform of Eq. (7a) and substituting the result into Eq. (2a), we obtain

$$\frac{1}{\sigma}\frac{\partial}{\partial \sigma}(\sigma^2Q_1) = \frac{1}{\sigma}\frac{\partial}{\partial \sigma}\left(\sigma\frac{\partial A}{\partial \sigma}\right)$$

Integrating this equation, we obtain

$$Q_1 = \frac{1}{\sigma}\frac{\partial A}{\partial \sigma} + \frac{f(x_1)}{\sigma^2} \tag{8a}$$

where $f(x_1)$ is an arbitrary function of x_1. Operating in a similar manner on Eqs. (7b) and (2b), we obtain the result

$$Q_1 = \frac{1}{\sigma}\frac{\partial A}{\partial \sigma} + g(\sigma) \tag{8b}$$

A comparison of Eqs. (8a) and (8b) shows that the most general relationship is

$$Q_1 = \frac{1}{\sigma}\frac{\partial A}{\partial \sigma} + \frac{c}{\sigma^2}$$

where c is a constant. Furthermore, to avoid unacceptable behavior in the correlations as x approaches zero, we must set

$c=0$. Thus, we obtain

$$Q_1=\frac{1}{\sigma}\frac{\partial A}{\partial \sigma} \tag{8c}$$

The corresponding relationship between Q_2 and B will now be derived. In order to obtain results containing only the variables x_1 and σ, we consider the sum $(R_{22}+R_{33})$. Thus transforming Eqs. (7c) and (7d) and equating with Eqs. (2c) and (2d), we obtain,

$$\frac{1}{\sigma}\frac{\partial}{\partial \sigma}\left(\sigma\frac{\partial A}{\partial \sigma}+\sigma\frac{\partial B}{\partial \sigma}\right)+2\frac{\partial^2 A}{\partial x_1^2}=\frac{1}{\sigma}\frac{\partial}{\partial \sigma}(2\sigma^2 Q_1+\sigma^2 Q_2)$$
$$+2\frac{x_1}{\sigma}\frac{\partial^2}{\partial x_1 \partial \sigma}(\sigma^2 Q_1)-\frac{x_1^2}{\sigma}\frac{\partial}{\partial \sigma}\left(\sigma\frac{\partial Q_1}{\partial \sigma}\right)-\sigma^2\frac{\partial^2 Q_1}{\partial x_1^2}$$

Using Eq. (8c) to combine the last terms on the right- and left-hand sides, we obtain after integration with respect to σ

$$Q_1+Q_2=\frac{1}{\sigma}\frac{\partial B}{\partial \sigma}+\frac{\partial^2 A}{\partial x_1^2}-2x_1\frac{\partial Q_1}{\partial x_1}+\frac{x_1^2}{\sigma}\frac{\partial Q_1}{\partial \sigma}+\frac{f(x_1)}{\sigma^2} \tag{9a}$$

Equating the expressions for R_{23} given by Eq. (2e) and the transform of Eq. (7e), and utilizing Eq. (8c) to eliminate $\partial^2 Q_1/\partial x_1^2$, we obtain after integration with respect to σ

$$Q_1+Q_2=\frac{1}{\sigma}\frac{\partial B}{\partial \sigma}+\frac{\partial^2 A}{\partial x_1^2}-2x_1\frac{\partial Q_1}{\partial x_1}+\frac{x_1^2}{\sigma}\frac{\partial Q_1}{\partial \sigma}+g(x_1) \tag{9b}$$

Comparison of Eqs. (9a) and (9b) shows that $f(x_1)$ and $g(x_1)$ must be identically zero.

Equations (8) and (9) will be used in Sec. IV to develop constraints which Q_1 and Q_2 must satisfy.

III. Application of Cramer's Theorem

In this section we derive constraints which the invariant functions of the energy spectrum tensor, $F(k_1,k_t)$ and $G(k_1,k_t)$, must satisfy. To do this we use a theorem developed by Cramer[17] which gives the necessary and sufficient conditions for $R_{ij}(\boldsymbol{x})$ to be the correlation tensor of a continuous stationary random process. These conditions are that $\Phi_{ij}(\boldsymbol{k})$ is integrable and that the quadratic form $\Phi=\zeta_j\zeta_k^*\Phi_{jk}$ is nonnegative for an arbitrary choice of the complex constants $\zeta_j=\xi_j+i\eta_j$ (the asterisk denotes the complex conjugate). The first condition insures that the integral defining R_{ij} converges. The second condition can be interpreted as the requirement that the energy spectrum associated with the velocity in an arbitrary direciton is positive for all values of the wave number.

The energy spectrum tensor Φ_{ij} is in general complex, but for the particular case of axisymmetric turbulence it can be shown to be real. Hence, in applying Cramer's theorem, we can assume without loss of generality that η_j is zero. Thus consider,

$$\Phi=\xi_i\xi_j f_{ij}F+\xi_i\xi_j g_{ij}G \tag{10}$$

where f_{ij} and g_{ij} are the coefficients of F and G in the expression for Φ_{ij} [see Eqs. (7)]. The problem of finding constraints on F and G then reduces to that of simultaneously diagonalizing two quadratic forms. The standard approaches for simultaneous diagonalization require one of the two matrices, $\boldsymbol{F}=[f_{ij}]$ and $\boldsymbol{G}=[g_{ij}]$, to be positive definite. In this case, both $\boldsymbol{F}$ and $\boldsymbol{G}$ are only positive semidefinite. However, it can be shown that if Rank $(\boldsymbol{F}|\boldsymbol{G})=$ Rank $(\boldsymbol{F})$, then an equivalent expression for the quadratic form Φ is

$$\Phi=y^T\hat{F}yF+y^T\hat{G}yG \tag{11}$$

where $\hat{\boldsymbol{F}}$ is a positive definite matrix and the dimension of the vector $\boldsymbol{y}$ is equal to Rank$(\boldsymbol{F})$. (The superscript T indicates the transpose.)

To apply this result to Eq. (10), we can simply calculate the orthogonal transformation $\xi=\boldsymbol{K}y$ which diagonalizes $\boldsymbol{F}$. Since the eigenvalues of $\boldsymbol{F}$ are $\lambda_1=\lambda_2=k^2$ and $\lambda_3=0$, y_3 does not appear in the quatratic form $y^T\boldsymbol{K}^T\boldsymbol{F}\boldsymbol{K}y$. Applying the same transformation to the second quadratic form, we find that y_3 does not appear here either. (This result could have been anticipated from the continuity equation, see Ref. 18.) Thus, we have achieved a representation in the form of Eq. (11), which can easily be diagonalized. Using an orthogonal transformation, $y=\boldsymbol{L}z$, we obtain

$$\Phi=z_1^2(k^2F+k_t^2G)+z_2^2k^2F \tag{12}$$

For the quadratic form Φ to be nonnegative, we must require

$$F(k_1,k_t)\geq 0 \tag{13a}$$

and

$$k^2F(k_1,k_t)+k_t^2G(k_1,k_t)\geq 0 \tag{13b}$$

for all values of the variables k_1 and k_t. Equations (13a) and (13b) will be used in the next section to derive constraints on $Q_1(\boldsymbol{x})$ and $Q_2(\boldsymbol{x})$.

IV. Constraints on Q_1 and Q_2

In Sec. II, we derived equations relating Q_1 and Q_2 to the Fourier transforms $A(x_1,\sigma)$ and $B(x_1,\sigma)$ of the energy spectrum functions F and G. These equations will be used to derive constraints on Q_1 and Q_2.

First consider the constraint on Q_1. From Eq. (8c) we see that we must examine $(1/\sigma)\partial A/\partial\sigma$. Expressing A as the Fourier transform of $F(\boldsymbol{k})$ and differentiating under the integral sign, we obtain

$$Q_1=\int_{-\infty}^{\infty}\int_0^{\infty}\int_0^{2\pi}\frac{ik_t\cos\theta}{\sigma}Fe^{i(k_1x_1+k_t\sigma\cos\theta)}k_t\,d\theta\,dk_t\,dk_1 \tag{14}$$

The integral over θ can be explicitly evaluated[19] to obatin

$$Q_1=-2\pi\int_{-\infty}^{\infty}\int_0^{\infty}\frac{J_1(\sigma k_t)}{\sigma k_t}e^{ik_1x_1}k_t^3F(k_1,k_t)\,dk_t\,dk_1 \tag{15}$$

It can be shown that $J_1(\alpha)/\alpha$ is maximized at $\alpha=0$ where it equals ½. Thus by virtue of Eq. (13a), we see that Q_1 must satisfy the inequality

$$Q_1(x_1,\sigma)\geq Q_1(0,0) \tag{16}$$

The second constraint which involves Q_2 will now be derived. Taking the Fourier transform of Eq. (13b), we obtain the constraint

$$\alpha(x_1,\sigma)\geq\alpha(0,0) \tag{17a}$$

where

$$\alpha(x_1,\sigma)=\frac{\partial^2 A}{\partial x_1^2}+\frac{1}{\sigma}\frac{\partial}{\partial\sigma}\left(\sigma\frac{\partial A}{\partial\sigma}\right)+\frac{1}{\sigma}\frac{\partial}{\partial\sigma}\left(\sigma\frac{\partial B}{\partial\sigma}\right) \tag{17b}$$

Using Eqs. (8) and (9), we can rewrite the function α in terms

of Q_1 and Q_2,

$$\alpha=\frac{2}{\sigma}\frac{\partial}{\partial\sigma}(\sigma^2Q_1)+\frac{1}{\sigma}\frac{\partial}{\partial\sigma}(\sigma^2Q_2)-\frac{x_1^2}{\sigma}\frac{\partial}{\partial\sigma}\left(\sigma\frac{\partial Q_1}{\partial\sigma}\right)$$

$$+2\frac{x_1}{\sigma}\frac{\partial^2}{\partial x_1\partial\sigma}(\sigma^2Q_1)-\frac{\partial^2}{\partial x_1^2}(\sigma^2Q_1)-\frac{\partial^2A}{\partial x_1^2} \tag{18}$$

Expressing A as the Fourier Transform of $F(\boldsymbol{k})$ and differentiating under the integral sign, we see from Eq. (13a) that

$$\frac{\partial^2A}{\partial x_1^2}\geq\frac{\partial^2A}{\partial x_1^2}\Big|_{x=0} \tag{19}$$

Adding Eqs. (17) and (19), we obtain

$$\beta(x_1,\sigma)\geq\beta(0,0) \tag{20a}$$

where

$$\beta=\frac{2}{\sigma}\frac{\partial}{\partial\sigma}(\sigma^2Q_1)+\frac{1}{\sigma}\frac{\partial}{\partial\sigma}(\sigma^2Q_2)-\frac{x_1^2}{\sigma}\frac{\partial}{\partial\sigma}\left(\sigma\frac{\partial Q_1}{\partial\sigma}\right)$$

$$+2\frac{x_1}{\sigma}\frac{\partial^2}{\partial x_1\partial\sigma}(\sigma^2Q_1)-\frac{\partial^2}{\partial x_1^2}(\sigma^2Q_1) \tag{20b}$$

Thus we see that the correlation tensor functions, Q_1 and Q_2, for axisymmetric turbulence are not entirely arbitrary, but must satisfy the constraints Eqs. (16) and (20). Whereas Eqs. (13) are necessary and sufficient conditions, Eqs. (16) and (20) are only necessary conditions. For a correlation function, the necessary and sufficient condition involves a convolution-type double integral[17] and is very difficult to test. Thus simpler constraints, such as Schwarz inequalities, are generally examined. Equations (16) and (20) represent a generalization of the Schwarz inequalities.

To see the relationship, note that the autocovariance of the velocity component in the direction of the unit vector ξ_i is given by $R(\boldsymbol{x})=\xi_i\xi_jR_{ij}(\boldsymbol{x})$. The associated energy spectrum is given by Eq. (10). The constraints Eqs. (16) and (20) are equivalent to requiring $R(\boldsymbol{0})\geq R(\boldsymbol{x})$ for all possible directions ξ_i. This is a stricter inequality than the standard Schwarz inequalities $R_{\alpha\alpha}(\boldsymbol{0})\geq R_{\alpha\alpha}(\boldsymbol{x})$ and $R_{\alpha\alpha}(\boldsymbol{0})R_{\beta\beta}(\boldsymbol{0})\geq R_{\alpha\beta}(\boldsymbol{x})$ (summation not implied). For example, choosing $\xi_1=\xi_2=1$, $\xi_3=0$ leads to $R(\boldsymbol{x})\leq R_{11}(\boldsymbol{0})+R_{22}(\boldsymbol{0})+R_{12}(\boldsymbol{0})+R_{21}(\boldsymbol{0})$. In the result obtained from the Schwarz inequalities, $R_{12}(\boldsymbol{0})+R_{21}(\boldsymbol{0})$ is replaced by the larger quantity $2\sqrt{R_{11}(\boldsymbol{0})R_{22}(\boldsymbol{0})}$. The constraints also have an advantage over the standard Schwarz inequalities in that they are applied directly to the invariant functions Q_1 and Q_2. Considering the complexity of Eqs. (2), the application of Eqs. (16) and (20) is much simpler than the task of deriving the correlations and applying the Schwarz inequalities individually.

Recently, the importance of realizability conditions has also received the attention of second-order turbulence modelers.[6] For that application, only the values of the correlations at $\boldsymbol{x}=0$ are of concern. Schumann[20] and du Vachat[21] have shown that, in addition to the Schwarz inequalities, the constraint $\mathrm{Det}[R_{ij}(\boldsymbol{0})]\geq 0$ must be enforced to assure realizability. The present constraints are somewhat more general in that nonzero values of $\boldsymbol{x}$ are considered. The appropriate constraints at $\boldsymbol{x}=0$ are also contained in Eqs. (16) and (20).

For isotropic turbulence, Q_1 is a function of $r=(x_1^2+\sigma^2)^{1/2}$ and Q_2 is zero. Equations (16) and (20) can be shown to be redundant in this case. Similarly, $F(\boldsymbol{k})$ depends only on the magnitude of $\boldsymbol{k}$ and $G(\boldsymbol{k})$ being zero. Thus, Eqs. (13) are also redundant for the case of isotropic turbulence.

V. Applications of Constraints

In this section, applications of axisymmetric turbulence theory to aerodynamic noise prediction are discussed. The examples are chosen to illustrate the value of the constraints [Eqs. (13), (16) and (20)]. Two important noise sources involving turbulence are high-speed jets and aircraft engine turbomachinery. In the case of jets, the noise is generated by the fluctuating Reynolds stresses, which are generally anisotropic. When aircraft engine fans are tested in static facilities, ingested atmospheric turbulence can produce substantial noise levels. The ingested turbulence is highly anisotropic due to the lateral contraction of the flow as it enters the inlet. Axisymmetric turbulence theory has been used to examine the importance of turbulence anisotropy for these two noise sources.

The prediction of aerodynamic noise is in general a very difficult task and a number of approximations must be made to make the problem tractable. In view of these approximations, a fairly crude turbulence model which minimizes algebraic complexity is typically employed. Often, the decay of the turbulence correlation in a given direction is modeled as $e^{-y/\ell}$, where ℓ is a turbulence integral length scale. This is, of course, unrealistic in terms of its behavior at both small and large values of y. However, it can be argued that the errors introduced by this deficiency are probably no worse than those resulting from the other approximations, and that reasonable results may be obtained for general trends such as the effect of length scale on noise level.

We will examine the predictions resulting from the use of two different axisymmetric turbulence models. Both of the models utilize

$$Q_1=-(u_a^2/2)e^{-y} \tag{21a}$$

$$y=\left(\frac{x_1^2}{\ell_a^2}+\frac{\sigma^2}{\ell_t^2}\right)^{1/2} \tag{21b}$$

The expressions for the second arbitrary function are

$$Q_2^{\mathrm{A}}=(u_a^2-u_t^2)e^{-y} \tag{22a}$$

$$Q_2^{\mathrm{B}}=-u_a^2\left[\left(\frac{u_t}{u_a}\right)^2-1+\frac{1}{2y}\left(\frac{x_1}{\ell_a}\right)^2\left(2-\frac{\ell_t^2}{\ell_a^2}-\frac{\ell_a^2}{\ell_t^2}\right)\right]e^{-y} \tag{22b}$$

Here u_a,ℓ_a and u_t,ℓ_t are the turbulence rms velocities and integral length scales in the axial and tangential directions, respectively. The models A and B appear equally reasonable in that they both produce the one-dimensional correlations $R_{11}(x_1)=u_a^2e^{-|x_1|/\ell_a}$ and $R_{22}(x_2)=u_t^2e^{-|x_2|/\ell_t}$. Model A might be preferred because the expression for Q_2 is simpler, but this is balanced by the fact that model B has the simpler form [for $G(\boldsymbol{k})$] in spectrum space. The predictions of fan noise and jet noise for these two models will be compared, concentrating on the case where $\ell_a/\ell_t>1$. As this ratio is increased, model A violates the constraints while model B remains valid. For large values of ℓ_a/ℓ_t, there are substantial differences between the noise levels predicted using models A and B, and arguments will be presented which show that the predictions based on model A are incorrect.

The prediction of fan noise caused by inflow turbulence will be discussed first. When aircraft engines are tested in static facilities, a substantial amount of noise is generated as a result of ingested atmospheric turbulence. Due to the large contraction of the inlet flow in the cross-stream direction, the turbulence which impinges on the fan is highly anisotropic. An analytical model of this noise source including the effects of anisotropy has recently been presented by Kerschen and Gliebe.[14] Here we ill concentrate on the importance of turbulence model realizability. Readers interested in details of the acoustic calculation should consult Ref. 14. The tur-

bulence axis of symmetry is assumed to be parallel to the fan inlet axis, and the correlations are measured in a reference frame moving with the uniform mean flow. The characteristic frequency of the turbulence in the moving frame is so small, compared to the fan blade passing frequency, that the correlations can be considered as functions of separation distance (x) alone.[12]

A summary of the available in-flow turbulence data measured in fan noise experiments is presented in Ref. 22. Typical conditions are $u_t/u_a=3$ and $\ell_a/\ell_t=300$. Thus, a suitable turbulence model should satisfy the constraints when $\ell_a/\ell_t \gg 1$. Since Eq. (16) is trivially satisfied by both models, we will concentrate attention on Eq. (20). For model A, calculating $\beta(x_1,\sigma)$ and taking the limit $\ell_a/\ell_t \gg 1$ (while keeping the magnitudes of x_1, σ, u_a, and u_t arbitrary), we find

$$\beta^A(x_1,\sigma)-\beta^A(0,0)=2u_t^2[1-e^{-y}]+u_t^2\frac{e^{-y}}{y}\left(\frac{\sigma}{\ell_t}\right)^2$$
$$-\frac{u_a^2}{2}\frac{e^{-y}}{y}\left[\left(\frac{x_1}{\ell_a}\right)^2 2\frac{\ell_a^2}{\ell_t^2}+\left(\frac{\sigma}{\ell_t}\right)^2\frac{\ell_t^2}{\ell_a^2}\right.$$
$$\left.-\left(\frac{x_1}{\ell_a}\right)^2\left(\frac{\sigma}{\ell_t}\right)^2\left(\frac{1}{y}+\frac{1}{y^2}\right)\frac{\ell_a^2}{\ell_t^2}\right]$$

In order to satisfy Eq. (20), the right-hand side of this expression must be non-negative for all choices of x_1 and σ. It can be shown that the worst case occurs for $\sigma=0$. Examining this case, we find that the constraint [Eq. (20)] is satisfied for all values of x_1 only if $u_t\ell_t/u_a\ell_a \geq 1/\sqrt{2}$. The experimental conditions quoted above ($u_t\ell_t/u_a\ell_a=0.01$) clearly violate this inequality. Thus, the application of the constraints has shown that model A is not a suitable representation for the inflow turbulence.

We will now examine the suitability of model B. Applying the constraint Eq. (20), we obtain the result

$$\beta^B(x_1,\sigma)-\beta^B(0,0)=2u_t^2(1-e^{-y})+u_a^2\left(\frac{\ell_t}{\ell_a}\right)^2\left(\frac{x_1}{\ell_a}\right)^2\frac{e^{-y}}{y}$$
$$+\left(u_t^2-\frac{u_a^2}{2}\frac{\ell_t^2}{\ell_a^2}\right)\left(\frac{\sigma}{\ell_t}\right)^2\frac{e^{-y}}{y}$$

The worst case for model B is $x_1=0$, which leads to the constraint $u_t\ell_a/u_a\ell_t \geq 1\sqrt{6}$. A surprising result is that ℓ_a/ℓ_t appears in the constraint for model B, as opposed to ℓ_t/ℓ_a in that for model A. This result is not easily anticipated from Eqs. (22). The experimental conditions typical of highly contracted flows ($\ell_a/\ell_t \gg 1$) easily meet the constraint for model B. For example, the data quoted above give $u_t\ell_a/u_a\ell_t=900$. Thus, we expect that the use of model B may lead to realistic predictions of inflow turbulence fan noise, while model A is likely to produce erroneous results. Calculations will be presented to show that this is indeed the case.

To ascertain the importance of constraint violations, fan noise calculations were performed for a range of turbulence parameters using both models A and B. The general trends observed in the parametric calculations are illustrated by the case $u_t=u_a$. For this case, Eq. (20) leads to the following constraints:

$$\text{model A,}\quad 1/\sqrt{6}<\ell_a/\ell_t<2$$
$$\text{model B,}\quad 1/\sqrt{6}<\ell_a/\ell_t<\infty \qquad (23)$$

Figure 1 shows the predicted sound power spectra in the vicinity of the fan blade passing frequency for a range of length scale ratios, $\ell_a/\ell_t=1.0$, 1.75, and 5.0. The axial length scale normalized by fan blade spacing was held fixed at

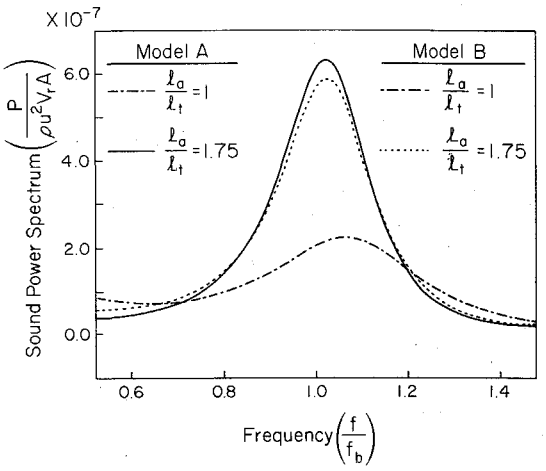

Fig. 1a Fan sound power spectrum predictions for cases where both models satisfy the constraints (normalizing factors are density, turbulence intensity, and fan relative velocity, frontal area, and blade passing frequency).

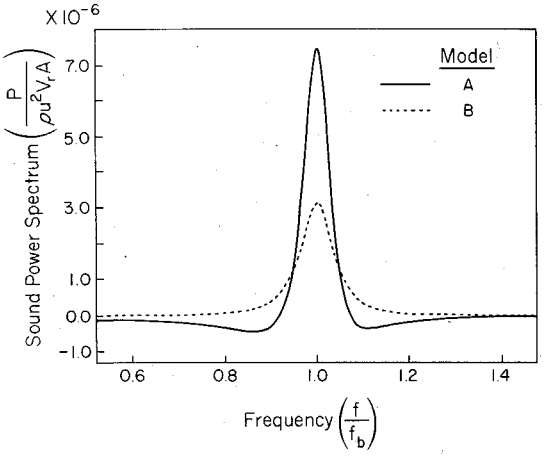

Fig. 1b Fan sound power spectrum predictions for $\ell_a/\ell_t=5$, where model B satisfies the constraints but model A does not.

$\ell_a/s=10$. The case $\ell_a/\ell_t=1.75$ is compared to the isotropic case in Fig. 1a. The predictions of models A and B are identical for isotropic turbulence ($\ell_a/\ell_t=1$). The introduction of moderate turbulence anisotropy ($\ell_a/\ell_t=1.75$) produces a substantial rise in the sound power generation, with the spectrum peak value increasing by approximately a factor of three. Both models satisfy the constraints when $\ell_a/\ell_t=1.75$, and the difference in the predictions of models A and B are fairly small compared to the large change from the $\ell_a/\ell_t=1$ case.

The predicted fan noise spectra for $\ell_a/\ell_t=5$ are shown in Fig. 1b. In this case, model B satisfies the constraints while model A does not. Here the differences in the predictions of models A and B are substantial, with the spectrum peak values differing by more than a factor of two. These differences continue to grow as ℓ_a/ℓ_t is increased. We also note that the sound power spectrum predicted for model A contains regions of "negative energy" on both sides of the fan blade passing frequency. This result is obviously physically incorrect and can be traced directly to the violation of the constraints. Essentially, the fan scatters the component of turbulent velocity normal to the blades When the constraints are violated, this velocity component is generally not realizable. It might be argued that a simple fix could be applied to correct this situation, such as setting the negative portions of the power spectrum to zero or taking the absolute value. However, applying such an approach to the spectrum for model A would produce noise levels far in excess of those predicted for model B, by as much as *three orders of*

magnitude at the experimentally measured conditions of $u_t/u_a = 3$, $\ell_a/\ell_t = 300$. The sound power predictions based on model B for $\ell_a/\ell_t \gg 1$ are in reasonable agreement with experimental data, as was shown in Ref. 14. Thus we must conclude that, for $\ell_a/\ell_t \gg 1$, the fan noise predictions based on model A are seriously in error.

We will now discuss the influence of turbulence anisotropy on jet noise. Goldstein and Rosenbaum[11] used the axisymmetric turbulence theory to examine this question. Their analysis is basically an application of the Lighthill[23] theory incorporating retarded time effects according to Ffowcs Williams.[24] Thus, the theory does not account for the shrouding of the source by the jet mean flow but is in other respects a suitable model for jet mixing noise. Since the present discussion is focused on the effects of turbulence model realizability, we consider Goldstein's formulation to be adequate.

Equation (47) of Goldstein and Rosenbaum gives the overall intensity $I(\boldsymbol{r},\boldsymbol{y})$ at a farfield observation point $\boldsymbol{r}$ due to a unit volume of turbulence at the source point $\boldsymbol{y}$. The source is essentially a fourth-order space-time velocity correlation tensor, where the time and spatial dependence $(\tau,\boldsymbol{x})$ is expressed in a coordinate system moving with the local turbulence convection velocity. The turbulence is assumed to be locally homogeneous. The overall intensity is related to the fourth-time derivative (evaluated at $\tau=0$) of certain weighted components of this velocity correlation tensor and can be separated into self-noise and shear-noise contributions.

In order to obtain detailed predictions, Goldstein and Rosenbaum employed model A for the spatial dependence of the turbulence correlations in the moving reference frame, while the time dependence in this frame was specified by a multiplicative function $f(\tau)$. The final result is given by their Eq. (52). This equation indicates that the effect of turbulence anisotropy on the farfield radiation pattern can be quite significant. Unfortunately, for some of the cases where the effects are largest, the turbulence model does not satisfy the constraints.

The importance of the constraint violations will be examined by comparing Goldstein's predictions to those obtained using model B. Goldstein and Rosenbaum's shear noise calculation indicates that anisotropy in turbulence length scale has a large effect on the farfield radiation pattern. Their Fig. 3 illustrates the shear noise directivity in terms of a plot of the quantity

$$D = \frac{\text{lateral quadrupole strength}}{\text{longitudinal quadrupole strength}}$$

for a range of ℓ_a/ℓ_t and turbulence symmetry axis orientations. The turbulence is assumed to be equal in all directions $(u_a = u_t)$. The effect of anisotropy $(\ell_a \neq \ell_t)$ is most pronounced when the turbulence axis of symmetry is aligned with the direction of the mean flow, i.e., the axial direction. For this orientation, the algebra is also considerably simplified. Thus we will consider this case in detail.

The shear noise contribution to the overall intensity can be written as

$$I_{sh}(\boldsymbol{r}|\boldsymbol{y}) = \frac{\rho_0 \cos^2\theta}{4\pi^2 c_0^5 (1-M_c\cos\theta)^5 r^2}\left[\cos^2\theta L_{11}(\boldsymbol{y}) + \sin^2\theta\sin^2\gamma L_{33}(\boldsymbol{y})\right] \tag{24a}$$

where θ and γ are the polar and azimuthal angles of the observation point relative to the jet axis. M_c is the eddy convection Mach number. The longitudinal and lateral quadrupole strengths ($i=1$ and 3, no summation convention) are given by

$$L_{ii}(\boldsymbol{y}) = \left[\frac{\partial^4}{\partial\tau^4}\int U\left(y_2 - \frac{1}{2}x_2\right)U\left(y_2 + \frac{1}{2}x_2\right) f(\tau) R_{ii}(\boldsymbol{x}|\boldsymbol{y})\,\mathrm{d}\boldsymbol{x}\right]_{\tau=0} \tag{24b}$$

where the mean velocity $U(y)$ is in the y_1 direction and depends only on y_2. The two point space-time turbulence correlation has been represented by separate time- and space-dependent factors. Assuming that the mean velocity gradient U' is constant over the turbulence correlation distance in the x_2 direction, we obtain the simple result

$$L_{ii} = -\frac{1}{4} f^{(iv)}(0) U'^2 \int x_2^2 R_{ii}(\boldsymbol{x})\,\mathrm{d}\boldsymbol{x} \tag{25}$$

When the turbulence axis of symmetry is aligned with the direction of the mean flow (x_1 coordinate direction), the R_{ii} in Eq. (25) are given directly by Eqs. (2). Utilizing Eqs. (21) and (22), evaluating the required integrals, and setting $u_t = u_a = u$, we obtain the following shear-noise longitudinal and latteral quadrupole strengths for models A and B,

$$L_{11}^{A,B} = C \tag{26a}$$

$$C = 8(\pi\ell_a\ell_t^2) f^{(iv)}(0)(uU'\ell_t)^2 \tag{26b}$$

$$L_{33}^{A} = C(\ell_a/\ell_t)^2 \tag{26c}$$

$$L_{33}^{B} = C(2 - \ell_t^2/\ell_a^2) \tag{26d}$$

The constant C is essentially the product of the correlation volume, an integration over frequency, and the strength of the turbulence/mean-shear interaction.

The quantity $D = L_{33}/L_{11}$ is a measure of the nonuniformity of the farfield radiation pattern. For large values of this ratio, the noise is radiated mainly in the transverse direction. Setting $\ell_a/\ell_t = 1+\epsilon$, we obtain the expansion $D = 1 + 2\epsilon + 0(\epsilon^2)$, valid for both models A and B. Thus the two models give identical results for small departures from isotropy. However, for large values of ℓ_a/ℓ_t, there are significant differences between the models. Model A predicts $D = (\ell_a/\ell_t)^2$, while model B predicts a monotonic increase to a maximum value of two. Thus, it is important to determine which model is most appropriate for large values of ℓ_a/ℓ_t.

The relative applicability of models A and B is most easily examined by using the constraints. The case under consideration is $u_a = u_t$, for which the constraints produce the inequalities [Eq. (23)]. In this case model A violates the constraints for $\ell_a/\ell_t \geq 2$, and the severity of the violation increases with ℓ_a/ℓ_t. Model B satisfies the constraints for arbitrarily large values of ℓ_a/ℓ_t. Thus, it is clear that the prediction of model B is most appropriate for large ℓ_a/ℓ_t. Goldstein and Rosenbaum's calculations,[11] which correspond to model A, significantly overpredict the nonuniformity in shear-noise radiation pattern due to axial length scales which are much larger than the transverse scale.

As further support for the jet noise predictions based on model B, it can be shown that for axisymmetric turbulence, the asymptotic value $D=2$ is independent of the exact shape of the transverse correlation curve. We consider the case $\ell_a \to \infty$ with fixed ℓ_t and $u_a = u_t$. Then there is complete correlation in the axial direction and we must consider the noise generated per unit axial length. The correlation functions depend only on (x_2, x_3), and the condition $u_a = u_t$ is achieved by setting $Q_2 = 0$, which corresponds to $F(\boldsymbol{k}) = G(\boldsymbol{k})$.

We then obtain from Eqs. (2)

$$R_{11}(x_2,x_3) = -2Q_1 - \sigma\frac{dQ_1}{d\sigma} \tag{27a}$$

and

$$R_{33}(x_2,x_3) = -2Q_1 - 2x_2\frac{\partial Q_1}{\partial x_2} \tag{27b}$$

where Q_1 is an arbitrary function of σ. Evaluating L_{11} and L_{33} from Eq. (25), we find (after appropriate integration by parts)

$$L_{11} = -(\pi/2)f^{(iv)}(0)U'^2\hat{Q} \quad \text{and} \quad L_{33} = 2L_{11}$$

where

$$\hat{Q} = \int_0^\infty \sigma^3 Q_1(\sigma)\,d\sigma$$

Thus, the asymptotic value $D=2$ is a general result not dependent on the exact shape of the transverse correlation curve. Although the limit $\ell_a \to \infty$ is somewhat artificial, this result indicates that the behavior predicted by model B is quite reasonable and that model A severely overestimates the nonuniformity in shear-noise radiation pattern due to unequal length scales ($\ell_a \gg \ell_t$).

The examples discussed in this section illustrate the value of the constraints [Eqs. (13), (16), and (20)]. Particular expressions for the correlation tensor functions $Q_1(x)$ and $Q_2(x)$ [or $F(k)$ and $G(k)$] have only limited ranges of applicability rather than being arbitrarily valid. The use of turbulence models which violate the constraints may produce quite unrealistic results. For the fan noise predictions, the nonrealizable turbulence model produced regions of "negative energy" in the frequency spectrum. Thus, in this case, there was an obvious clue that the predictions were incorrect. Application of the constraints to the turbulence model would have identified the problem prior to use of the model. On the other hand, in the jet noise calculation based on model A, there appeared to be no reason to question the results, except that rather large effects were predicted. It seems, in fact, that the results shown here to be incorrect have not been previously disputed. Thus, in jet noise prediction, application of the constraints would have indicated the likelihood of a significant error, an error which is not easily identified by other means.

VI. Summary

In his development of the axisymmetric turbulence theory, Chandrasekhar showed that the velocity correlation tensor R_{ij} could be expressed in terms of two invariant functions, $Q_1(x_1,\sigma)$ and $Q_2(x_1,\sigma)$. However, his development used only kinematic and symmetry requirements to deduce the form of R_{ij}. In the present paper, we have shown that, for R_{ij} to be the correlation tensor of a continuous stationary random process, certain constraints must be imposed upon Q_1 and Q_2 . The corresponding invariant functions $F(k_1,k_t)$ and $G(k_1,k_t)$ in the energy spectrum tensor must also satisfy a set of constraints.

The constraints are particularly useful for applications of axisymmetric turbulence theory to the modeling of turbulent flow by-products. Most calculations of this nature have assumed isotropic turbulence, for which the realizability conditions are relatively straightforward. However, to obtain more accurate predictions, the turbulence anisotropy may have to be accounted for. There are also some flows that are so highly anisotropic that realistic predictions cannot be obtained without including this feature. One example is ingested turbulence in ground-based fan test facilities. In these situations axisymmetric turbulence is an attractive alternative to the isotropic model. The arbitrary functions of axisymmetric turbulence must then be given assumed forms. However, the greater flexibility of the axisymmetric turbulence model adds to the difficulty of choosing appropriate forms which satisfy the realizability conditions. The constraints developed in this paper provide a systematic approach for determining the range of validity of a particular formulation.

To illustrate the value of the constraints, axisymmetric turbulence theory was used to examine the effect of turbulence anisotropy on fan noise and jet noise. In both of these cases, the use of a turbulence model which violated the constraints led to serious errors in prediction. The error in the jet shear-noise calculation was not easily discerned by examining the incorrect prediction, but was identified by using the constraints and by comparison with alternative models. The present results indicate that, for $\ell_a/\ell_t \gg 1$, Goldstein and Rosenbaum's[11] model significantly overpredicts the nonuniformity in shear-noise radiation pattern due to unequal length scales.

Acknowledgments

This work was supported financially by the NASA Ames Research Center under Contract NAS2-10002. I would like to thank Dr. T.F. Balsa for useful discussions during the course of the study.

References

[1] Taylor, G. I., "Statistical Theory of Turbulence," *Proceedings of the Royal Society of London,* Ser. A, Vol. 151, 1935, p. 421.

[2] Taylor, G. I., "The Spectrum of Turbulence," *Proceedings of the Royal Society of London,* Ser. A, Vol. 164, 1939, p. 176.

[3] von Kármán, T., "On the Statistical Theory of Turbulence," *Proceedings of the National Academy of Science,* Vol. 23, 1937, p. 98.

[4] von Kármán, T., "The Fundamentals of the Statistical Theory of Turbulence," *Journal of the Aeronautical Sciences,* Vol. 4, 1937, p. 131.

[5] von Kármán, T. and Howarth, L., "On the Statistical Theory of Isotropic Turbulence," *Proceedings of the Royal Society of London,* Ser. A, Vol. 164, 1938, p. 192.

[6] Lumley, J. L., "Computational Modeling of Turbulent Flows," *Advances in Applied Mechanics,* Vol. 18, 1978, pp. 124-176.

[7] Herring, J. R., "Approach of Axisymmetric Turbulence to Isotropy," *Physics of Fluids,* Vol. 17, 1974, pp. 859-872.

[8] Schumann, U. and Patterson, G. S., "Numerical Study of the Return of Axisymmetric Turbulence to Isotropy," *Journal of Fluid Mechanics,* Vol. 88, 1978, pp. 711-735.

[9] Sreenivasan, K. R. and Narasimha, R., "Rapid Distortion of Axisymmetric Turbulence," *Journal of Fluid Mechanics,* Vol. 84, 1978, pp. 497-516.

[10] Hassan, Y. A., Jones, B. G., and Adrian, R. J., "Measurements and Axisymmetric Model of Spatial Correlations in Turbulent Pipe Flow," *AIAA Journal,* Vol. 18, 1980, pp. 914-920.

[11] Goldstein, M. E. and Rosenbaum, B. M., "Effect of Anisotropic Turbulence on Aerodynamic Noise," *Journal of the Acoustical Society of America,* Vol. 54, 1973, pp. 630-645.

[12] Goldstein, M. E., Rosenbaum, B. M., and Albers, L. V., "Sound Radiation from a High-Speed Axial-Flow Fan Due to the Inlet Turbulence Quadrupole Interaction," NASA TN D-7667, June. 1974.

[13] Mani, R. and Bekofske, K., "Experimental and Theoretical Studies of Subsonic Fan Noise," NASA CR-2660, 1976.

[14] Kerschen, E. J. and Gliebe, P. R., "Noise Caused by the Interaction of a Rotor with Anisotropic Turbulence," *AIAA Journal,* Vol. 19, June 1981, pp. 717-723.

[15] Batchelor, G. K., "The Theory of Axisymmetric Turbulence," *Proceedings of the Royal Society of London,* Ser. A, Vol. 186, 1946, pp. 480-502.

[16] Chandrasekhar, S., "The Theory of Axisymmetric Turbulence," *Philosophical Transactions of the Royal Society of London,* Ser. A, Vol. 242, 1950, pp. 557-577.

[17] Cramer, H., "On the Theory of Stationary Random Processes," *Annals of Mathematics,* Vol. 41, 1940, pp. 215-230.

[18] Batchelor, G. K., *Theory of Homogeneous Turbulence,* Cambridge University Press, London, 1956, pp. 27-28.

[19] Abramowitz, M. and Stegun, I., *Handbook of Mathematical Functions,* Dover Publications, New York, 1973, p. 360.

[20] Schumann, U., "Realizability of Reyonlds Stress Turbulence Models," *Physics of Fluids,* Vol. 20, 1977, pp. 721-725.

[21] DuVachat, R., "Realizability Inequalities in Turbulent Flows," *Physics of Fluids,* Vol. 20, 1977, pp. 551-556.

[22] Gliebe, P. R. and Kerschen, E. J., "Analytical Study of the Effects of Wind Tunnel Turbulence on Turbofan Rotor Noise," NASA CR 152359, 1979, p. 37.

[23] Lighthill, M. J., "On Sound Generated Aerodynamically: I. General Theory," *Proceedings of the Royal Society of London,* Ser. A, Vol. 211, 1952, pp. 564-587.

[24] Ffowcs Williams, J. E., "The Noise from Turbulence Convected at High Speed," *Philosophical Transactions of the Royal Society of London,* Ser. A, Vol. 255, 1963, p. 469.